IJCRT.ORG ISSN : 2320-2882

INTERNATIONAL JOURNAL OF CREATIVE RESEARCH THOUGHTS (IJCRT)

An International Open Access, Peer-reviewed, Refereed Journal

Experimental Investigation On The Flexural Behavior Of Cold-Formed Steel Built-Up Composite Beams Infilled And Encased With Eps-Based Lightweight Concrete

[1]A.S. Elsonpaty, [2]Wael R. A. Ibrahim, [2]Mohamed M. Yehia [3]Fatouh M. F. Shaker

[1]Research Assistant, [2]Assistant Professor, [3]Assistant Professor, [4]Professor

[1]Civil Engineering Department,

[1]Faculty of Engineering at Mataria, Helwan University, 11718, Cairo, Egypt

Abstract: This paper presents an experimental investigation into the flexural performance of built-up cold-formed steel (CFS) closed-section beams under four-point bending, with a focus on the effect of composite action using Expanded Polystyrene Lightweight Concrete (EPS-LWC). Three full-scale beams were examined: a bare steel built-up section and two composite variants utilizing the same steel cross-sectional area. The first composite beam (Beam-2) was fully infilled and externally encased with EPS-LWC to assess the contribution of composite interaction. The second composite beam (Beam-3) included a novel configuration featuring outward-facing lipped flanges embedded within the concrete matrix, intended to enhance mechanical interlock and strain transfer. Experimental results showed that EPS-LWC encasement significantly improved the flexural capacity, stiffness, and ductility of the CFS beam. Moreover, Beam-3 demonstrated superior performance over Beam-2, attributed to improved interface bonding and strain compatibility through the lipped flange interlock. These findings confirm the structural viability of EPS-LWC for composite steel applications and highlight the potential of flange detailing innovations in maximizing composite action in thin-walled CFS members.

***Index Terms*:** Cold-formed steel (CFS), EPS-LWC, composite action, flexural behavior, lipped flange interlock, lightweight concrete, built-up beams.

I. INTRODUCTION

Cold-formed steel (CFS) sections have gained substantial attention in the construction industry due to their favorable mechanical properties, including high strength-to-weight ratio, ease of fabrication, and cost-efficiency. Their use is particularly prevalent in lightweight structural systems such as secondary framing, roof trusses, wall panels, and floor joists. However, the thin-walled geometry of CFS sections also introduces critical limitations—most notably, their susceptibility to various forms of buckling, including local, distortional, and lateral-torsional buckling under flexural and axial loads. This vulnerability becomes especially pronounced in built-up members where the stability of individual plates and screw-fastened assemblies governs performance (Dubina et al., 2013; Schafer & Peköz, 1998).

Recent advances in composite construction offer promising pathways to mitigate these instabilities. One such strategy involves the integration of cold-formed steel sections with lightweight concrete (LWC), where the concrete serves as both a structural component and a bracing medium for the thin steel walls. This composite action reduces local deformations, enhances flexural stiffness, and increases load-carrying capacity (Yu & LaBoube, 2010; Shanmugam & Lakshmi, 2001). Among various LWC types, Expanded Polystyrene Lightweight Concrete (EPS-LWC) has emerged as an attractive solution due to its reduced density, thermal insulation properties, and utilization of recycled materials. Research by Lam et al. (2018), Shi et al. (2016),

and Salahaldeen & Al-Hadithi (2022) has demonstrated that EPS-LWC mixtures can achieve compressive strengths in the range of 15–30 MPa with densities below 1.6 t/m³, making them ideal for composite structural applications where weight reduction is crucial.

Despite the clear benefits of EPS-LWC, one of the major challenges in achieving effective composite interaction is the bond strength at the steel–concrete interface. Cold-formed steel surfaces, which are typically smooth and thin, offer limited interfacial friction and adhesion—especially in the absence of dedicated shear connectors. Previous studies (Wright et al., 2018; Zhou & Uy, 2015) have reported premature debonding and localized slip as dominant failure modes in steel–LWC composite beams, particularly when exposed to flexural loading. While adhesive bonding or mechanical fasteners are commonly proposed solutions, they often present challenges in practical construction involving thin CFS plates or retrofitted systems.

To address this issue, recent innovations have explored the potential of geometric interlock features such as lips, grooves, or corrugations that can passively enhance bond behavior. In cold-formed construction, the lipped channel section is widely used for its improved local buckling resistance. However, its application as a means for enhancing composite interaction remains underutilized. Embedding the lipped flanges into lightweight concrete encasement may allow them to act as integral shear-transfer mechanisms within the composite section. This approach not only increases mechanical bond but also improves confinement around the compression flange, thereby reducing instability. Studies such as Yan et al. (2016) and Oehlers & Bradford (1999) have indicated the promise of such detailing in improving structural ductility and delaying failure in composite systems.

The current research focuses on the flexural performance of three full-scale built-up closed-section CFS beams tested under four-point bending. Beam 1 serves as a bare steel control, while Beam 2 incorporates EPS-LWC as infill and encasement to evaluate the improvement due to composite action. Beam 3, which uses the same steel section, introduces a novel design by orienting the CFS lips outward and fully embedding them within the concrete encasement to function as mechanical interlocks. This design aims to enhance the strain transfer mechanism between steel and concrete and prevent premature debonding.

This paper presents detailed experimental observations including load–deflection response, strain distribution, failure modes, and cracking patterns. The results validate the role of EPS-LWC in improving stiffness and capacity and demonstrate that the novel lipped flange detailing significantly enhances composite interaction, thereby offering a robust and sustainable solution for cold-formed steel applications.

II. EXPERIMENTAL PROGRAM

2.1 Overview

The experimental investigation focused on understanding the flexural behavior of cold-formed steel (CFS) built-up beams in bare and composite conditions using expanded polystyrene lightweight concrete (EPS-LWC). Three full-scale beams were fabricated using the same steel cross-sectional area, each tested under four-point bending. Beam 1 served as the bare steel reference; Beam 2 was a standard composite beam filled and encased with EPS-LWC; and Beam 3 shared the same steel geometry as Beam 2 but included outward-facing lipped flanges embedded in the concrete to enhance mechanical interlock. This program included a full material testing campaign, structural fabrication, strain instrumentation, casting and curing of LWC, and the execution of full-scale flexural testing.

2.2 Beam Configuration and Section Design

All beams were fabricated using cold-formed steel (CFS) channels with a nominal thickness of 2 mm, formed from S275JR steel sheets. A dedicated material testing campaign was carried out to confirm the steel properties. Flat tensile coupons cut from the web and flange zones were tested according to ASTM E8/E8M procedures. The average yield strength was 315.1 MPa, and the modulus of elasticity was 197634.6 MPa, ensuring consistency in mechanical performance across all specimens.

The channels were connected face-to-face through their flanges using self-drilling screws spaced at 50 mm longitudinally. This screw spacing was selected based on connection design criteria specified in Yu & LaBoube (2010) to ensure complete shear transfer between the components of the built-up section. The two

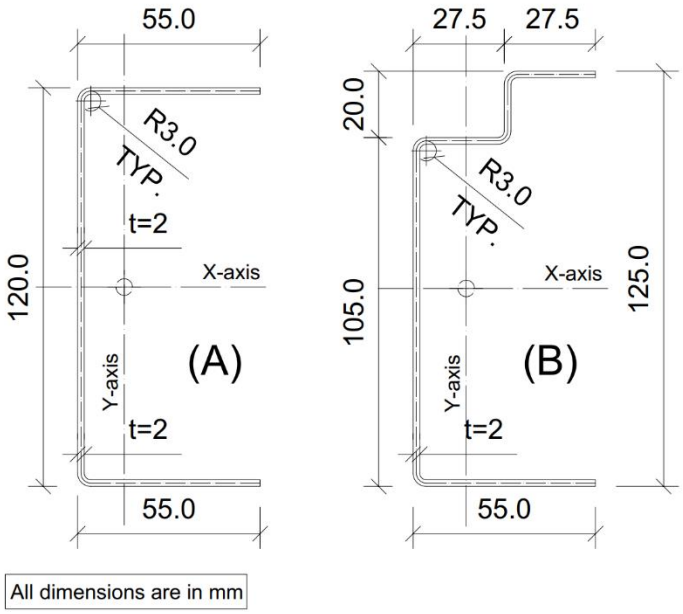

Figure 1: Cross-sections of the individual cold-formed steel channels: plain and lipped profiles.

channel types used—plain and lipped—are shown in Figure 1, while their respective built-up configurations are illustrated in Figure 2.

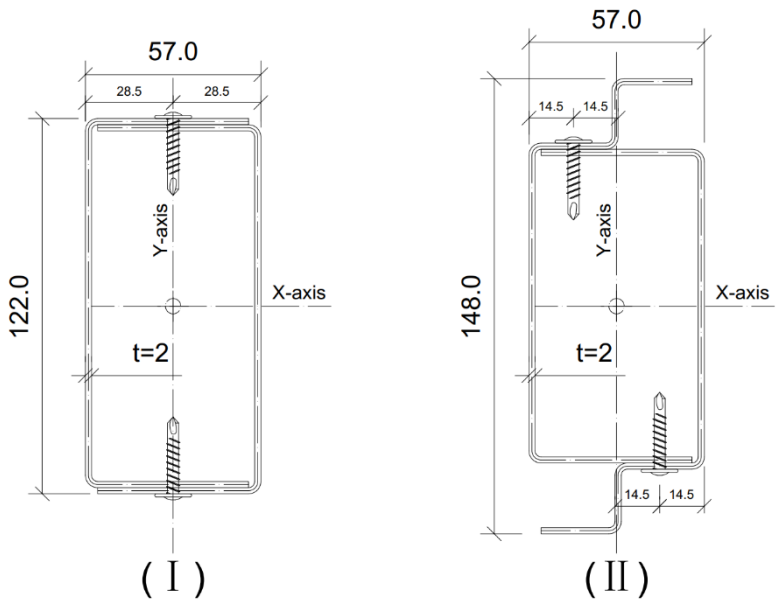

Figure 2: Built-up CFS sections: (left) used in Beams 1 & 2; (right) used in Beam 3.

Figure 3: Timber fill inside Beam 1 used to prevent crippling without affecting flexural behavior.

Beam 1 (bare steel) and Beam 2 (standard composite) used the same plain CFS built-up section. Beam 3 used the same steel area but employed outward-facing lipped flanges, embedded into the surrounding EPS-LWC to promote mechanical bond. To simulate the internal restraint typically provided by concrete in hollow steel sections, Beam 1 was internally braced with a tightly-fitted timber fill, as shown in Figure 3. This bracing

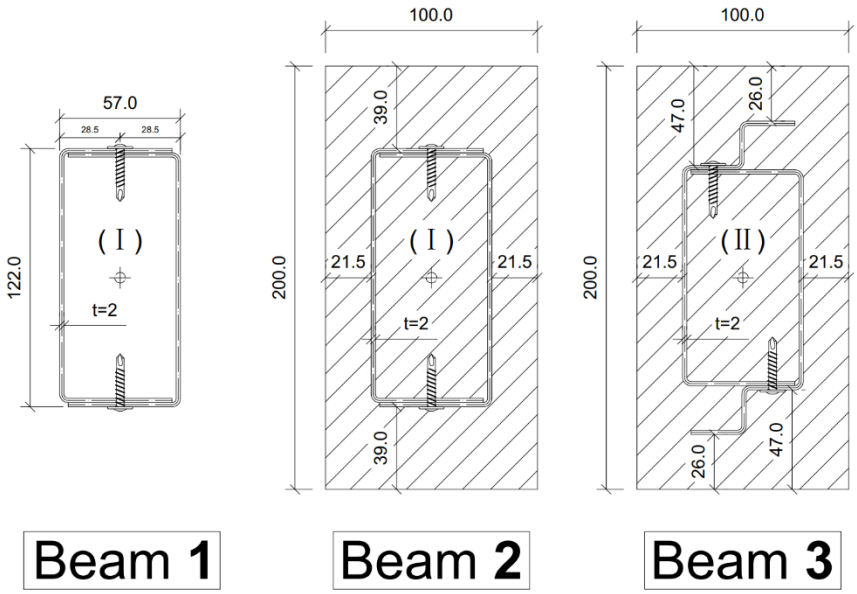

Figure 4: Final cross-sections of Beams 1, 2, and 3 in bare steel & composite conditions.

prevented inward flange buckling but did not contribute to load resistance. The final cross-sectional conditions of all three beams are depicted in Figure 4.

2.3 EPS-LWC Material Properties and Mix Design

To evaluate the mechanical performance of the expanded polystyrene lightweight concrete (EPS-LWC) used in the composite beams, a dedicated material testing campaign was conducted. The mix design replaced all coarse aggregate with recycled expanded polystyrene (EPS) beads, as shown in Figure 5, and included Portland cement, fly ash, silica fume, and a polycarboxylate-based superplasticizer. The resulting mix was highly flowable, self-compacting, and homogeneous, ensuring complete encapsulation of the steel section without segregation. A representative sample of the fresh EPS-LWC mixture is shown in Figure 6 during the slump test, which yielded a slump value of 200 mm.

As part of the validation process, Compressive strength tests have been conducted on both 150 × 150 × 150 mm cubes and 150 mm diameter × 300 mm cylinders. These tests followed standard procedures as per ASTM C39 and EN 12390-3. The average 28-day compressive strength of the cubes was found to be 25.28 MPa, while the corresponding cylinder strength was approximately 20.2 MPa, based on direct testing and supported by the typical empirical correction factor of 0.8 between cube and cylinder results. These values confirm that the EPS-LWC mix achieved sufficient strength for use in structural composite members.

In addition, the modulus of elasticity was determined from cylinder specimens and found to be 10.9 GPa, while the measured dry density of the hardened concrete was approximately 1.4 t/m³. These characteristics qualify the EPS-LWC as both a structurally effective and lightweight medium, contributing to reduced self-

Figure 5: Recycled expanded polystyrene (EPS) beads used as lightweight aggregate in the LWC mix.

Figure 6: Fresh EPS-based lightweight concrete in slump test showing self-compacting consistency.

weight and improved energy absorption under flexural loading. The combination of strength, stiffness, and sustainability makes this mix well-suited for use in cold-formed steel composite systems.

2.4 Instrumentation and Strain Gauge Setup

Each beam was instrumented with three strain gauges at mid-span to evaluate internal force distribution and composite interaction. The strain gauges were bonded at the following locations:

1. Bottom steel flange – for tension strain
2. Top steel flange – for compression strain
3. Top surface of LWC – for concrete compressive strain (in Beams 2 and 3)

Surface preparation included grinding and cleaning with acetone to ensure adequate bonding, and the gauges were covered with tape during casting to prevent moisture intrusion. The complete gauge layout across the section depth is shown in Figure 7, and actual installation conditions were carefully monitored throughout the process.

This instrumentation allowed for a detailed evaluation of strain compatibility between the steel and LWC

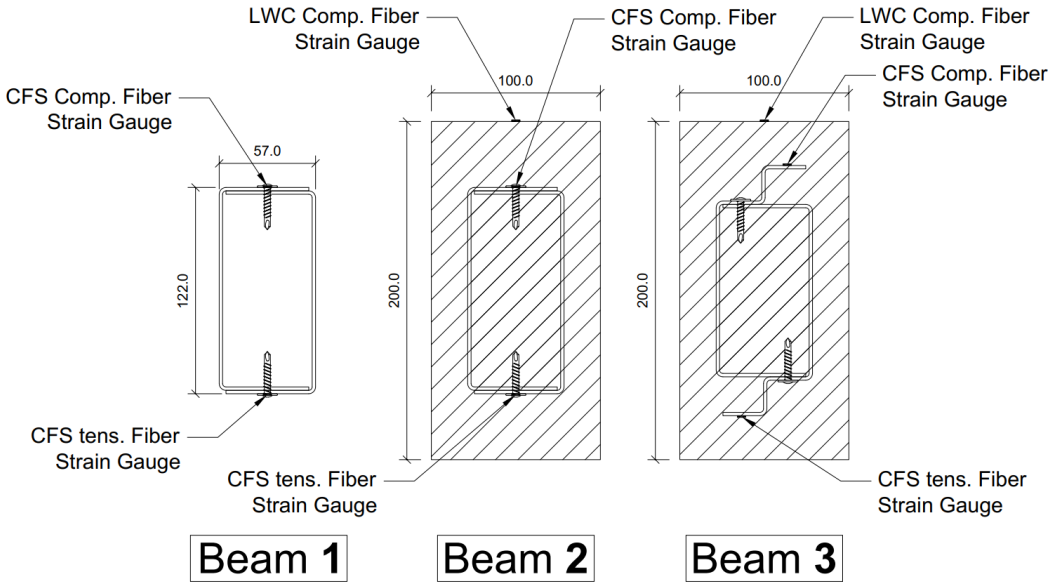

Figure 7: Strain gauge layout across the mid-span cross-section of Beams 1–3.

layers, as well as the detection of interface slip or debonding phenomena.

2.5 Beam Casting and Curing Procedures

Beams 2 and 3 were cast in custom timber molds that ensured consistent LWC cover thickness: 39 mm on top and bottom for beam 2, and 21.5 mm on both sides of the steel for beam 3. The steel sections were centrally fixed and braced within the formwork to prevent displacement during casting. The EPS-LWC mix was poured in two stages to facilitate proper encapsulation around the steel and minimize air entrapment. Due to its self-compacting nature, only minimal rodding was applied.

After casting, the beams were cured under wet burlap for 28 days, with manual water application twice per day to maintain saturation. This curing procedure ensured uniform hydration and proper development of compressive strength throughout the LWC. The complete casting and curing process was carefully monitored to replicate field-like conditions and ensure consistency across both composite beams.

2.6 Flexural Testing Methodology

All beams were tested under four-point bending with a clear span of 1800 mm. Two concentrated loads were applied symmetrically at one-third span intervals using a 1500 kN capacity hydraulic jack and spreader beam. Load was measured using a calibrated load cell. Displacement was recorded using two LVDTs located at mid-span and one-third span, while a dial gauge at mid-span was used to capture lateral deformation in Beam 1. Load was applied incrementally at 2 kN intervals until failure or significant post-peak capacity degradation was observed.

Strain data were recorded continuously using a multi-channel data acquisition system. Crack formation, deflection shape, and local failures were documented throughout the test. Photos of the beam setup before

Figure 8a: Beam 1 under four-point bending test setup.

testing for each specimen are presented in Figures 8a, 8b, and 8c, illustrating the consistency of the test configuration and boundary conditions.

III. RESULTS AND DISCUSSION

3.1 Load–Deflection Behavior

The load–deflection responses of Beams 1, 2, and 3 under four-point bending are presented in Figure 9. All beams exhibited the characteristic three-phase behavior typical of thin-walled CFS flexural members: an initial linear-elastic stage, a stiffness degradation phase due to local instabilities or interface slip, and a softening or plateau phase post-peak.

Beam 1, the bare steel section, demonstrated a linear response up to approximately 25 kN, after which a gradual stiffness reduction occurred due to the onset of local buckling in the compression flange and adjacent webs. The beam reached a peak load of 30.3 kN at a mid-span deflection of 8.63 mm, after which deformation localized, leading to a post-peak softening phase.

Beam 2, the composite section with EPS-LWC encasement, showed a stiffer response from the early stages due to the confining effect of the surrounding lightweight concrete. The linear range extended up to 45 kN before the first signs of interface debonding and diagonal cracking occurred. This beam achieved a peak load of 56.78 kN at a deflection of 11.67 mm, representing an 87% increase in load-carrying capacity compared to Beam 1. However, a noticeable drop in stiffness was observed post-peak, attributed to concrete cracking and bond failure along the steel–concrete interface.

Figure 8b: Beam 2 under four-point bending test setup.

Figure 8c: Beam 3 under four-point bending test setup.

Beam 3, featuring the same steel section but with outward-facing lipped flanges embedded in the EPS-LWC, exhibited the most enhanced flexural performance. The initial stiffness and overall load capacity were significantly higher than the other two beams. The beam reached a peak load of 86.48 kN at a deflection of 12.32 mm, representing a 185% increase over Beam 1 and 52% improvement over Beam 2. Unlike Beam 2, Beam 3 sustained its load capacity over a longer deflection range, suggesting improved post-peak ductility and strain compatibility between steel and concrete.

The overall comparison shown in Figure 9 highlights the critical role of composite action in improving both stiffness and strength, and demonstrates that the introduction of mechanical interlock via lipped flanges can

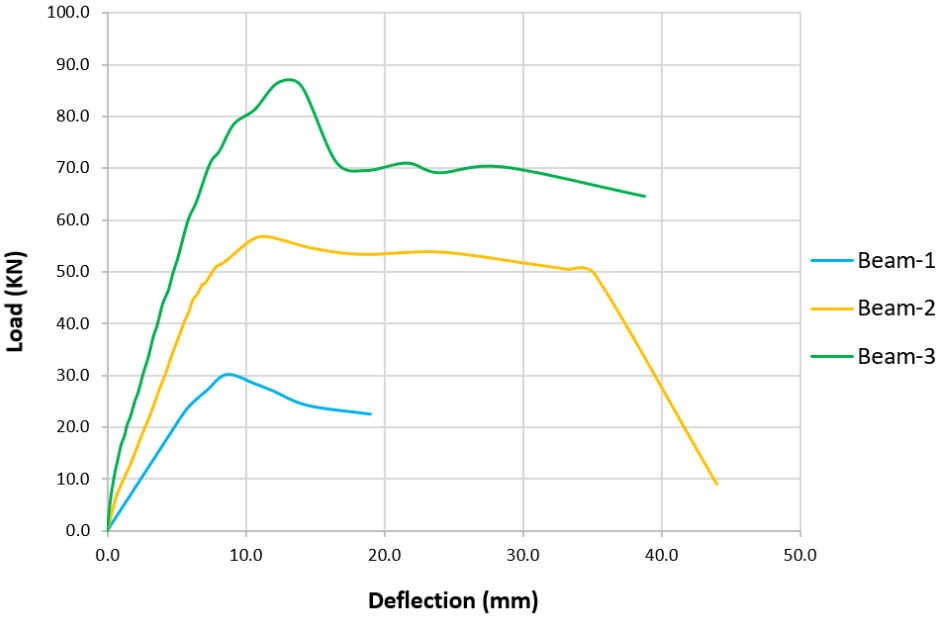

Figure 9: load–deflection curves of beams 1, 2, and 3 under four-point bending.

significantly reduce interfacial slip and delay failure.

3.2 Failure Modes and Crack Patterns

The failure mechanisms observed in Beams 1, 2, and 3 were distinct and closely related to their level of composite interaction and section configuration. Visual inspections and post-failure analysis revealed key differences in how each beam responded to flexural loading.

Beam 1 (bare steel) failed predominantly by local buckling of the compression flange and adjacent web plates near the mid-span region. Buckling occurred in the constant moment zone, where the top flange experienced the highest compressive stresses. No signs of lateral-torsional buckling were observed, owing to the closed box section and the presence of an internal timber filler, which provided effective lateral restraint without contributing to load resistance. This restrained the section's inward deformation and allowed the failure to develop in a more localized and symmetric manner. The deformation profile and flange buckling at peak load are clearly visible in Figure 10.

Beam 2 (standard composite with EPS-LWC) exhibited a different mode of failure, initiated by diagonal shear cracks and progressing into debonding at the steel–LWC interface. The cracks developed near the junction between the lightweight concrete encasement and the steel web and flanges. As the load increased, a gradual separation occurred between the steel and the LWC along the lower flange. Importantly, no concrete crushing was observed, suggesting that failure was dominated by interface slip rather than material over-stressing. This loss of bond reduced the effectiveness of composite action and allowed localized steel buckling to re-emerge. These characteristics are evident in Figure 11, which shows the shear cracking pattern and delamination of the lower steel flange from the concrete.

Beam 3 (composite with lipped flange interlock) exhibited the most stable and ductile failure behavior. The outward-facing lipped flanges embedded in the EPS-LWC acted as passive shear connectors, effectively restraining slip and ensuring full strain compatibility between the materials. Cracks developed gradually and remained widely distributed, mainly as diagonal flexural-shear cracks in the LWC. At peak load and beyond, concrete crushing was observed at the top compression zone, indicating that the concrete was fully engaged in flexural resistance. However, unlike Beam 2, there was no evidence of interface debonding, and the steel flanges remained fully bonded to the surrounding matrix throughout the test. These observations are

highlighted in Figure 12, which shows the integrity of the interlock and the crushed top surface of the EPS-LWC.

In conclusion, the progression of failure modes across the three beams confirms the increasing effectiveness

Figure 10: local buckling observed in beam 1 following flexural failure

Figure 11: Interface debonding and diagonal cracking in beam 2 under load.

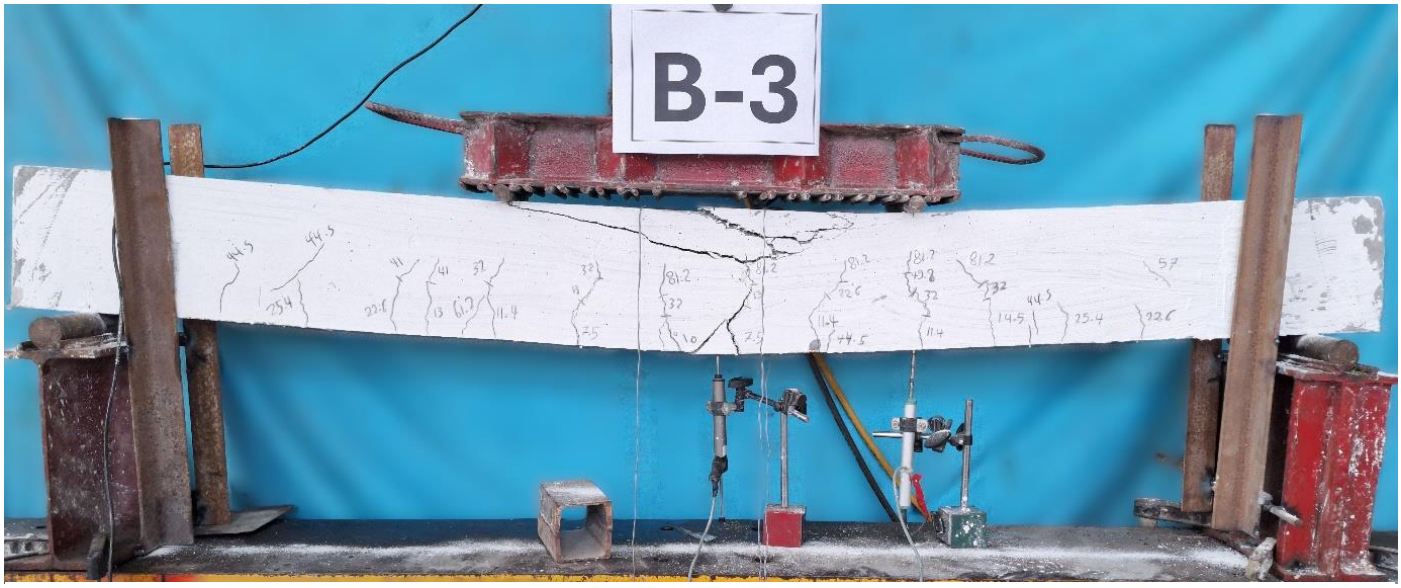

Figure 12: Concrete crushing and intact steel–concrete bond in beam 3 with lipped flange interlock.

of composite action—from unbraced steel in Beam 1, to partial bond in Beam 2, to full mechanical interlock in Beam 3. The presence of the lipped flange interlock in Beam 3 not only enhanced the ultimate capacity but

also delayed the onset of critical cracking and allowed the system to fail in a more ductile and predictable manner.

3.3 Strain Distribution and Composite Action

Strain measurements at the mid-span section were used to evaluate the degree of composite interaction and compatibility between the cold-formed steel (CFS) and the expanded polystyrene lightweight concrete (EPS-LWC). Three strain gauges were installed on each beam: one at the top flange of the steel (compression zone), one at the bottom flange (tension zone), and one on the top surface of the EPS-LWC in Beams 2 and 3. The results provide a direct comparison of strain evolution under increasing load and reveal how effectively the composite sections behaved as unified structural elements.

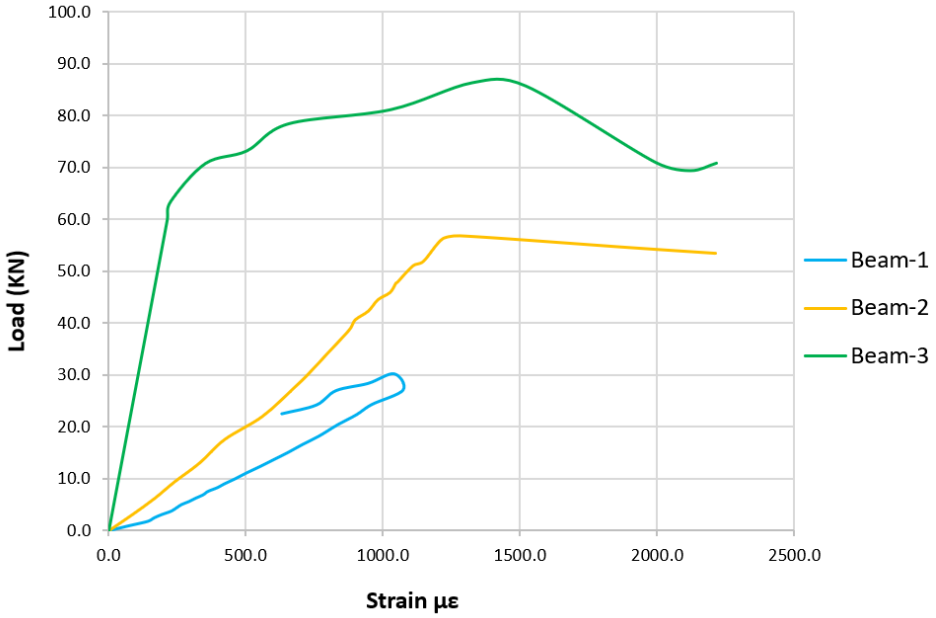

Figure 13: Compressive strain in the top flange of the CFS section for beams 1, 2, and 3.

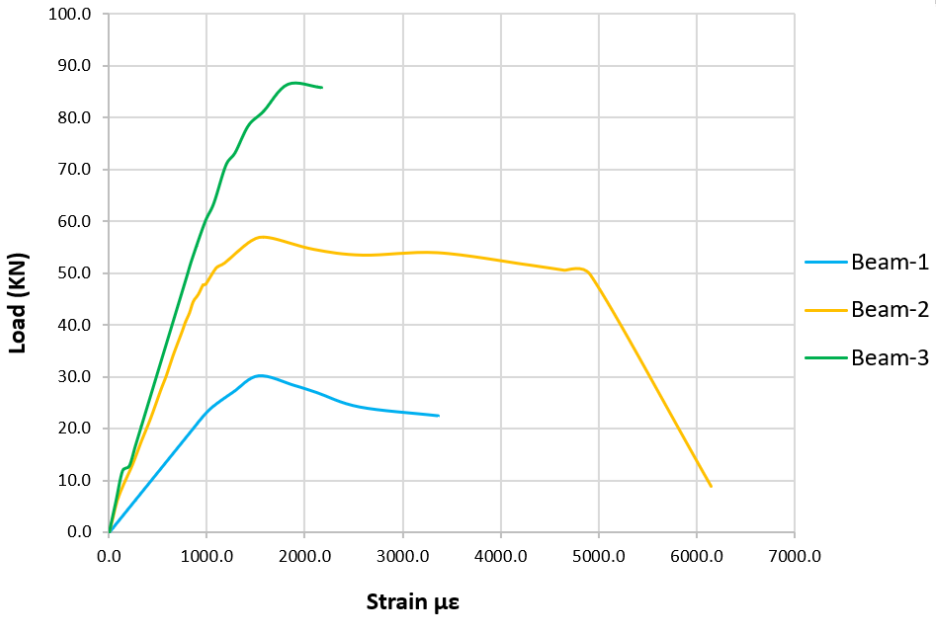

Figure 14: Tensile strain in the bottom flange of the CFS section for beams 1, 2, and 3.

The compressive strain in the top steel flange is shown in Figure 13. Beam 1, being a bare steel section, displayed a linear strain increase until flange buckling initiated near peak load. Beam 2 exhibited a slightly delayed compressive strain response, but a sharp transition occurred after bond degradation at the steel–concrete interface. Beam 3 demonstrated the most stable and extended compressive strain curve, indicating full utilization of the concrete's confining effect and enhanced interaction due to the lipped flange interlock.

The tensile strain at the bottom steel flange is shown in Figure 14. Beam 1, carrying the full tensile force in the steel, exhibited the highest strain magnitude. Beam 2 followed a similar trend initially but diverged post-cracking of the LWC. Beam 3 displayed the lowest tensile strain at peak load, confirming that a portion of the tensile stress was effectively transferred into the surrounding concrete — a direct result of improved bond and strain distribution offered by the interlock mechanism.

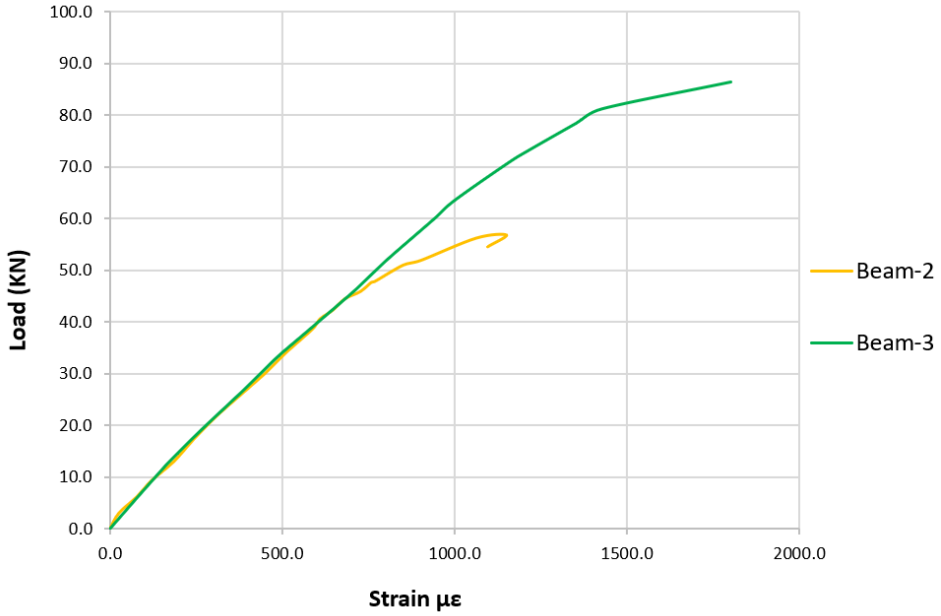

Figure 15: Compressive strain at the top surface of the EPS-LWC in beams 2 and 3.

The compressive strain in the EPS-LWC for Beams 2 and 3 is illustrated in Figure 15. Beam 2 reached a strain level close to the material's capacity but plateaued prematurely due to debonding between the concrete and the steel flange. No crushing was observed. In contrast, Beam 3 exhibited a higher peak strain and a more gradual increase, culminating in visible concrete crushing near the top surface. This clearly indicates that the concrete was fully engaged and resisted compressive stress up to failure — a hallmark of effective composite action.

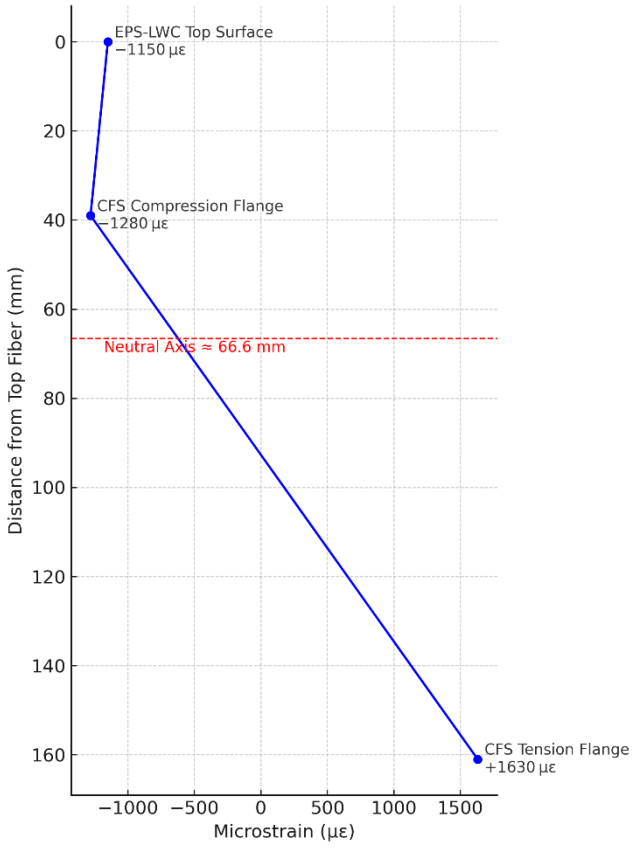

Figure 16: Strain compatibility distribution across the depth of beam 2 at peak load.

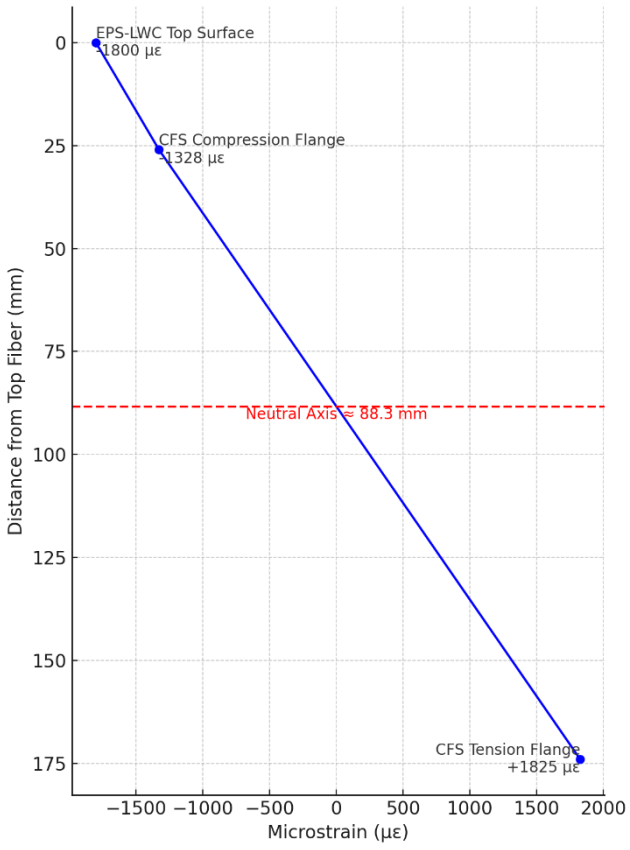

Figure 17: Strain compatibility distribution across the depth of beam 3 at peak load.

To further evaluate composite behavior, strain compatibility profiles were plotted at the mid-span section at peak load. These profiles assess the linearity of strain distribution through the section depth. Figure 16 shows the strain profile of Beam 2. While the data initially followed a linear trend, discontinuities near the concrete–steel interface reveal partial slip and loss of strain transfer — consistent with the debonding observed during testing. This confirms that Beam 2 achieved only partial composite interaction.

In contrast, Figure 17 shows the strain profile of Beam 3. Here, the distribution closely follows a linear gradient from top to bottom, confirming full strain compatibility and validating that the steel and concrete acted in unison. The presence of embedded lipped flanges clearly contributed to a stronger mechanical connection, preventing interface slip and maintaining force equilibrium throughout the section.

These results collectively confirm that Beam 3 achieved the highest level of composite action, both in terms of load sharing and strain coordination. Beam 2 benefited from concrete encasement but was limited by insufficient bond. Beam 1, as expected, acted as a non-composite steel section with independent tension and compression strain development.

3.4 Comparative Summary

To better quantify and visualize the performance enhancements provided by EPS-LWC infill and the lipped flange interlock, key flexural metrics were extracted from experimental results. These include the ultimate bending moment capacity and the initial flexural stiffness, which together illustrate both strength and serviceability improvements across the three beam types.

The ultimate moment capacity of each beam was calculated using the peak applied load and the constant moment arm of 0.6 m. As shown in Figure 18, Beam 1 (bare steel) exhibited a moment capacity of 18.17 kN·m. Upon the introduction of EPS-LWC in Beam 2, the moment increased significantly to 34.07 kN·m, representing an 87.5% increase. Beam 3, with embedded lipped flanges, reached the highest moment capacity of 51.89 kN·m, marking a 52.3% gain over Beam 2 and an overall improvement of 185.6% compared to Beam 1. These results clearly demonstrate that while composite action alone greatly enhances strength, the addition of a mechanical interlock further optimizes stress transfer and flexural capacity.

In terms of serviceability, the initial flexural stiffness—measured from the slope of the elastic portion of the load–deflection response—also showed notable gains, as illustrated in Figure 19. Beam 1 registered a stiffness of 4.13 kN/mm. Beam 2 increased to 7.4 kN/mm, an improvement of 79.1% due to the added lateral confinement and rigidity provided by the EPS-LWC. Beam 3 reached a peak stiffness of 10.6 kN/mm, showing a further 43.2% improvement over Beam 2. The enhanced stiffness in Beam 3 confirms that strain compatibility and interface integrity from the lipped flange detailing not only improved strength but also delayed deformation, making the system more resilient under service loads.

Together, these results highlight that:

- The transition from bare steel to composite construction nearly doubled both moment capacity and stiffness.
- The addition of the lipped flange interlock created a structurally superior system with improved composite interaction, crack control, and energy absorption.
- Beam 3 offers a promising configuration for lightweight, high-performance structural applications where weight savings and ductility are critical.

This comparative evaluation supports the conclusion that mechanically interlocked EPS-LWC composite

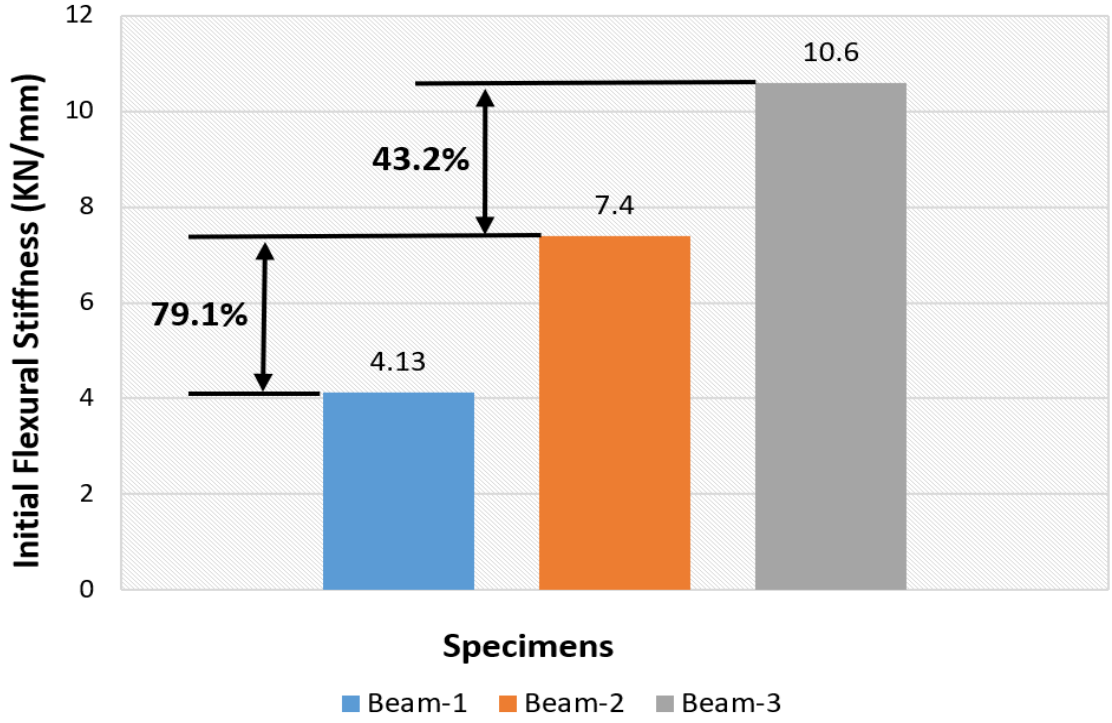

Figure 19: Initial flexural stiffness of beams 1, 2, and 3 based on the slope of the linear portion of the load–deflection response.

beams offer significant structural benefits beyond conventional composite systems.

3.4 Discussion of Composite and Interlock Effects

The experimental results from Beams 1, 2, and 3 clearly demonstrate the progressive improvements in flexural behavior achieved through the application of lightweight concrete (LWC) encasement and the novel lipped flange interlock system. These enhancements are the result of both material synergy and interface detailing, which together govern strain compatibility, stress redistribution, and failure modes in thin-walled built-up cold-formed steel (CFS) composite sections.

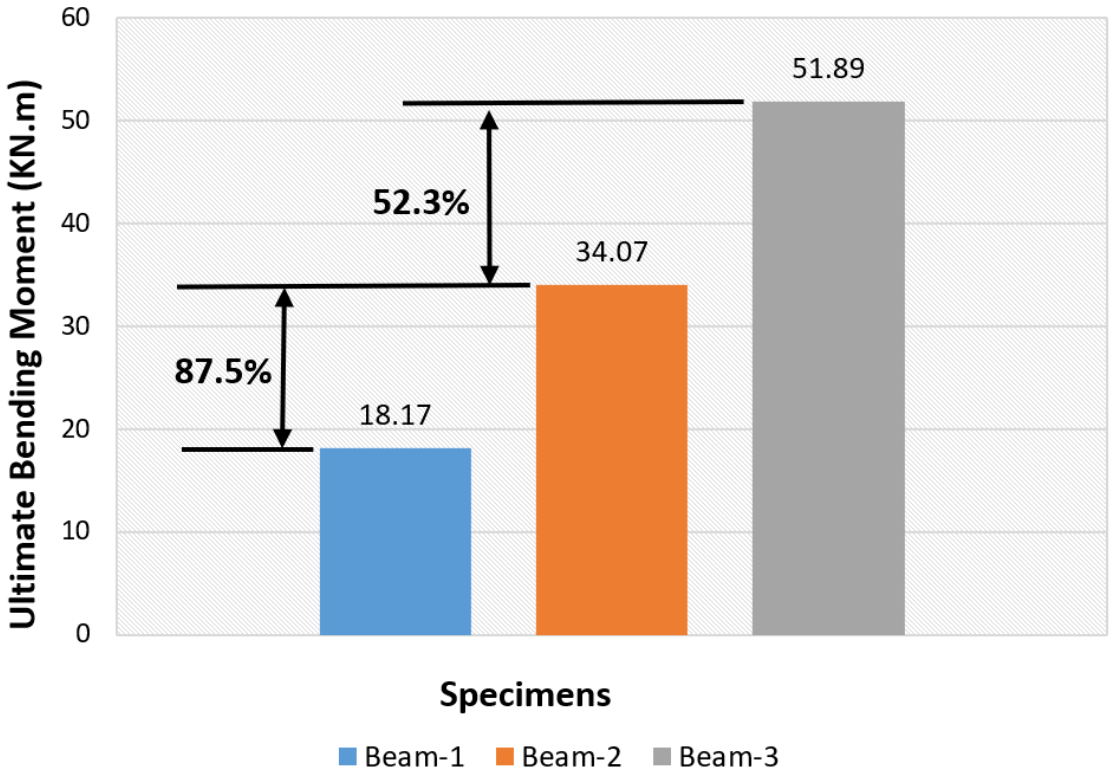

Figure 18: Ultimate flexural moment capacity of beams 1, 2, and 3 derived from peak load and effective moment arm.

Beam 2, incorporating conventional EPS-LWC infill and encasement, showed a substantial increase in both stiffness and strength over Beam 1. This confirms that even without mechanical connectors, the composite action arising from confinement and surface bond is sufficient to significantly mobilize the surrounding concrete. The concrete provided lateral support to the thin steel flanges, suppressed local buckling, and shared part of the compressive load. However, strain measurements and failure observations revealed a premature debonding between the steel and concrete once the strain in the LWC approached its compressive limit. This bond failure limited the effectiveness of composite action in the post-yield stage, leading to a drop in both ductility and ultimate strain capacity.

Beam 3, however, introduced a geometric interlock mechanism by orienting the lipped flanges outward and embedding them in the EPS-LWC. This passive interlock acted as a continuous shear-transfer system without requiring discrete connectors. The strain results for Beam 3 showed a near-linear distribution across the section depth and strong correlation between steel and concrete strains, indicating excellent strain compatibility and full composite behavior throughout the loading process. No debonding or slip was observed at failure, and instead, crushing of the concrete in the top fiber occurred — a desirable and predictable failure mode that confirms full stress development in the LWC. The increased moment capacity and stiffness recorded in Beam 3 were consistent with this full engagement.

Moreover, the interlock mechanism enhanced post-peak ductility, delayed crack localization, and extended the useful deformation range of the beam. These benefits are particularly important in applications where seismic resistance, impact loading, or fatigue life are critical considerations. By eliminating reliance on adhesive or mechanical connectors, the lipped flange system simplifies fabrication while providing robust interface behavior.

In summary, the findings of this study confirm that:

- EPS-LWC can serve as an effective infill and encasement material for CFS built-up sections.
- Composite action can be significantly enhanced by passive geometric interlock mechanisms.
- The proposed flange interlock system offers a simple, lightweight, and highly effective shear transfer strategy, capable of transforming the behavior of thin-walled CFS beams from localized instability-driven failure to ductile, distributed flexural performance.

These results not only validate the experimental hypotheses but also provide a practical design direction for future structural applications involving cold-formed steel and lightweight concrete composites.

IV. CONCLUSIONS AND RECOMMENDATIONS

This experimental study assessed the flexural behavior of three full-scale built-up cold-formed steel (CFS) box beams under four-point bending. Beam 1 was a bare steel section, Beam 2 was a conventionally encased composite beam using expanded polystyrene lightweight concrete (EPS-LWC), and Beam 3 utilized the same steel area but introduced a novel interlock system via outward-facing lipped flanges embedded within the concrete. Based on the observed flexural behavior, strain measurements, and failure modes, the following conclusions and recommendations are drawn:

1. EPS-LWC effectively enhances the flexural performance of thin-walled CFS beams. The composite Beam 2 demonstrated an 87.5% increase in moment capacity and a 79.1% increase in stiffness compared to the bare steel beam. This confirms the contribution of concrete infill and encasement to lateral restraint and load sharing.
2. The use of lipped flange interlock in Beam 3 significantly outperformed the conventional composite approach, yielding 185.6% higher moment capacity and 156.7% higher stiffness compared to the bare beam, and a 52.3% and 43.2% improvement over Beam 2, respectively.
3. Strain profiles revealed that Beam 2 experienced premature debonding, resulting in partial composite action. Beam 3 maintained full strain compatibility and showed crushing of the LWC, indicating complete and ductile composite behavior.
4. The interlock mechanism proved to be a simple, passive, and effective alternative to traditional shear connectors, requiring no welding or adhesives, and offering improved bonding and crack control under flexure.

Recommendations:

- Designers and fabricators of composite lightweight steel structures may adopt embedded flange interlock mechanisms for improved strength, stiffness, and structural efficiency.
- EPS-LWC is recommended for sustainable composite beam applications due to its favorable strength-to-weight ratio, energy absorption capacity, and recycled content.

V. FUTURE WORK

To build upon the findings of this research, the following future directions are suggested:

1. Conduct parametric studies varying flange lip dimensions, spacing, and embedment depth to optimize the mechanical interlock for different CFS geometries.
2. Evaluate long-term and dynamic behavior, including fatigue performance, cyclic loading, and seismic response, particularly for critical infrastructure applications.
3. Investigate the performance of partially filled or partially encased CFS beams, which may offer further material efficiency without compromising structural integrity.
4. Apply the interlock mechanism to open-section CFS configurations and hybrid composite systems to assess its generalizability across different structural forms.
5. Develop finite element models calibrated with experimental data to simulate composite action, predict failure progression, and guide future design practices.

VI. ACKNOWLEDGMENT

The author gratefully acknowledges the support provided by the Structural Materials Testing Laboratory and the Concrete Technology Laboratory at the Faculty of Engineering at Mataria, Helwan University, for their assistance in specimen preparation, material testing, and full-scale experimental work.

VII. REFERENCES

[1] Yu, W.-W., & LaBoube, R. A. (2010). *Cold-formed steel design* (4th ed.). John Wiley & Sons.

[2] American Society for Testing and Materials. (2020). *ASTM C39/C39M–20: Standard test method for compressive strength of cylindrical concrete specimens*. ASTM International.

[3] American Society for Testing and Materials. (2021). *ASTM E8/E8M–21: Standard test methods for tension testing of metallic materials*. ASTM International.

[4] American Society for Testing and Materials. (2022). *ASTM C796/C796M–22: Standard test method for foaming agents for use in producing cellular concrete using preformed foam*. ASTM International.

[5] Kankanamge, N. D., & Mahendran, M. (2011). Experimental studies of cold-formed steel beams with rectangular hollow flanges. *Thin-Walled Structures, 49*(12), 1543–1556.

[6] Pham, C. H., & Hancock, G. J. (2010). Numerical simulation of high strength cold-formed purlins in combined bending and shear. *Thin-Walled Structures, 48*(10), 727–738.

[7] Moen, C. D., & Schafer, B. W. (2011). Direct strength prediction of cold-formed steel beam–columns. *Journal of Structural Engineering, 137*(12), 1329–1338.

[8] Sukontasukkul, P., & Chaikaew, C. (2006). Properties of concrete pedestrian block mixed with crumb rubber. *Construction and Building Materials, 20*(7), 450–457.

[9] Soroushian, P., & Marikunte, S. (1992). Behavior of steel fiber reinforced concrete under direct tension. *ACI Materials Journal, 89*(6), 603–610.

[10] Aslani, F., & Nejadi, S. (2013). Self-compacting concrete incorporating steel and polypropylene fibers: compressive and tensile strengths, modulus of elasticity, shrinkage and impact resistance. *Construction and Building Materials, 53*, 121–133.